



ELSEVIER

Earth and Planetary Science Letters 196 (2002) 175–187

EPSL

www.elsevier.com/locate/epsl

## U–Th dating of marine isotope stage 7 in Bahamas slope sediments

Laura F. Robinson<sup>a,\*</sup>, Gideon M. Henderson<sup>a</sup>, Niall C. Slowey<sup>b</sup>

<sup>a</sup> Department of Earth Sciences, Oxford University, Parks Road, Oxford OX1 3PR, UK

<sup>b</sup> Department of Oceanography, Texas A&M University, College Station, TX 77843-3146, USA

Received 16 July 2001; received in revised form 10 December 2001; accepted 18 December 2001

### Abstract

In order to understand the driving forces for Pleistocene climate change more fully we need to compare the timing of climate events with their possible forcing. In contrast to the last interglacial (marine isotope stage (MIS) 5) the timing of the penultimate interglacial (MIS 7) is poorly constrained. This study constrains its timing and structure by precise U–Th dating of high-resolution  $\delta^{18}\text{O}$  records from aragonite-rich Bahamian slope sediments of ODP Leg 166 (Sites 1008 and 1009). The major glacial–interglacial cycles in  $\delta^{18}\text{O}$  are distinct within these cores and some MIS 7 substages can be identified. These sediments are well suited for U–Th dating because they have uranium concentrations of up to 12 ppm and very low initial  $^{230}\text{Th}$  contributions with most samples showing  $^{230}\text{Th}/^{232}\text{Th}$  activity ratio of  $>75$ . U and Th concentrations and isotope ratios were measured by thermal ionisation mass spectrometry and multiple collector inductively coupled plasma mass spectrometry, with the latter providing dramatically better precision. Twenty-nine of the 41 samples measured have a  $\delta^{234}\text{U}$  value close to modern seawater suggesting that they have experienced little diagenesis. Ages from 27 of the 41 samples were deemed reliable on the basis of both their U and their Th isotope ratios. Ages generally increase with depth, although we see a repeated section of stratigraphy in one core. Extrapolation of constant sedimentation rate through each substage suggests that the peak of MIS 7e lasted from  $\sim 237$  to 228 ka and that 7c began at 215 ka. This timing is consistent with existing low precision radiometric dates from speleothem deposits. The beginning of both these substages appears to be slightly later than in orbitally tuned timescales. The end of MIS 7 is complex, but also appears to be somewhat later than is suggested by orbitally tuned timescales, although this event is not particularly well defined in these cores. © 2002 Elsevier Science B.V. All rights reserved.

**Keywords:** interglacial environment; Th/U; Bahamas; inductively coupled plasma methods; paleoclimatology

### 1. Introduction

The chronology of Quaternary climate is gen-

erally based on orbital tuning (e.g. [1,2]) in which marine stratigraphic records are dated with reference to solar insolation at 65°N following Milankovitch [3]. Even though the same insolation curve has been used for tuning, there are differences in the timing and structure of change in the various tuned records depending on the exact tuning method used and on the records that were

\* Corresponding author.

Tel.: +44-1865-282-112; Fax: +44-1865-272-072.

E-mail address: laurar@earth.ox.ac.uk (L.F. Robinson).

tuned (e.g. Fig. 1). Although insolation and climate change are certainly closely linked their relationship is not a simple one. This complexity is most apparent at glacial terminations where the rapid melting of the ice sheets is clearly not a linear response to insolation forcing. To understand this complexity, orbitally tuned records have been calibrated using radiometric techniques (e.g. [4–6]). Such dating has shown that Termination I coincides with peak northern hemisphere summer insolation. In contrast, recent U–Th dating of Termination II shows that it preceded the peak of insolation by as much as 8 kyr [7,8]. If we

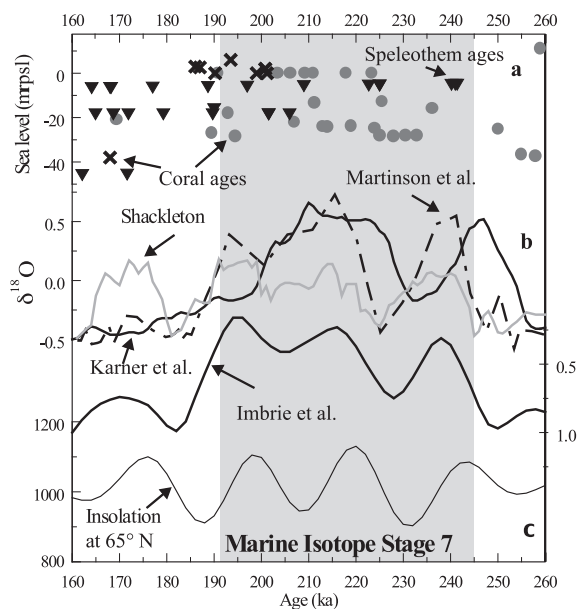


Fig. 1. Summary of existing data between 260 and 160 kyr. Grey shading represents the extent of MIS 7 following the timing of the Imbrie et al. tuned stratigraphy [1]. (a) shows U-series dates on carbonate rocks. Black triangles represent ages from speleothems ([27–31]) and sea level must be below these points. Crosses are from Barbados corals with  $\delta^{234}\text{U}$  that suggest they have not been diagenetically altered (in the range 135–165) [8,10,24,26]. Grey dots are from corals whose  $\delta^{234}\text{U}$  falls outside this range and whose ages are therefore considered unreliable [8,10,24,26,37–39]. (b) shows four tuned  $\delta^{18}\text{O}$  records: the SPECMAP curve measured on planktonic foraminifera in five deep-sea cores [1], a timescale based on benthic foraminifera from seven deep-sea cores [2] a new tuned curve based on benthic foraminifera [33] and a reconstruction of  $\delta^{18}\text{O}$  which is attributed to ice volume and sea-level changes only (Fig. 4A in [40]). (c) shows insolation changes calculated at  $65^\circ\text{N}$ .

are to understand the differences between these two terminations, and the relationship between insolation and climate change more generally, it is helpful to look further back in the climate record to marine isotope stage 7 (MIS 7).

The uranium series provides dating techniques that overlap the range of  $^{14}\text{C}$  dating ( $\sim 50$  ka) and extend to cover a significant portion of the Brunhes-chron [9]. Insolation peaks have a calculated periodicity of  $\sim 20$  kyr, so dating needs to have a resolution significantly better than  $\sim 10$  kyr if the phasing of climate and insolation is to be deduced. Thermal ionisation mass spectrometry (TIMS) U–Th dating has frequently been applied to coral samples and has provided high precision ages for the last 130 kyr (e.g. [4–6,10]). Older corals have also been dated but prove more difficult to date for two reasons. Firstly, the U–Th system tends to be diagenetically altered by meteoric waters when subject to multiple or lengthy episodes of subaerial exposure. Secondly,  $^{230}\text{Th}/^{238}\text{U}$  measurements need to be more precise since the change in ratio with age becomes smaller as time increases. Only a few MIS 7 corals have yielded precise ages that do not appear to have been affected by diagenesis. Speleothems can also be U–Th dated to provide sea level and U–Th age constraints from MIS 7. Combining existing U–Th dates from corals and speleothems does not, however, provide sufficient data to constrain the behaviour of climate and sea level during MIS 7, particularly during the early stages (Fig. 1).

This study aims to constrain the timing and structure of MIS 7 by precise U–Th dating of aragonite-rich Bahamian slope sediments that have never been subaerially exposed.

## 2. Sedimentary setting

The sediments used in this study are from ODP Leg 166, which sampled the leeward slope of the Great Bahamas Bank in 1996. The two cores examined, Core 1008 ( $23^\circ 36.64'\text{N}$ ,  $79^\circ 5.01'\text{W}$ , 437 m) and Core 1009 ( $23^\circ 36.84'\text{N}$ ,  $79^\circ 3.00'\text{W}$ , 308 m) are composed of unlithified aragonite-rich mudstones, wackestones and packstones [11].

The cores are well suited for the purposes of

this study. The advantages are two-fold: they have a detailed stratigraphy and are suitable for direct U–Th dating. The  $\delta^{18}\text{O}$  stratigraphy of bulk sediment and of the planktonic foraminifer, *Globigerinoides sacculifer*, show that the cores are substantially complete through the last few glacial–interglacial cycles. Interglacial periods have a particularly high-resolution record since flooding of the bank tops gives rise to rapid aragonite production. The aragonite is swept off the banks and onto the slopes by tidal processes. Sedimentation rates can be as high as 200 cm/kyr in these interglacial portions [12]. Glacial sections are relatively condensed because low sea level exposes the bank top slowing aragonite production and reducing the sedimentation rate.

The water depth of both cores (308 and 437 m) ensures that the sediments have not been subject to subaerial diagenesis since their deposition, even during times of low sea level. At the site of the deeper core, Core 1008, the slope is at a lower angle than Core 1009. Therefore, although Core 1008 has a lower sedimentation rate, it is less susceptible to stratigraphic disturbance.  $^{14}\text{C}$  ages confirm that ages in Core 1008 increase smoothly with depth during the Holocene [12]. Core 1009 shows more variable sedimentation, but the overall stratigraphy is still intact [12].

The high-stand portions of these cores can be dated directly by U–Th techniques on bulk sediment. The aragonite has U concentrations of up to 12 ppm causing radiogenic  $^{230}\text{Th}$  to be relatively abundant, and allowing U and Th isotope ratios to be measured precisely.  $^{230}\text{Th}$  has two sources in addition to radiogenic ingrowth. These sources are (a) detrital material and (b) scavenging of insoluble  $^{230}\text{Th}$  from the water column. In many deep-sea sediments these two sources overwhelm the ingrown thorium rendering the sediments useless for U–Th dating. In these Bahamian sediments, however, detrital content is extremely low, typically  $<1\%$  [13], minimising initial  $^{230}\text{Th}$ . In addition, the shallow water depth means that very little scavenging can take place as the sediments settle through the water column. The small contribution of initial  $^{230}\text{Th}$  to the measured value can readily be corrected when calculating ages.

### 3. Analytical methods

One gram of each sample was slowly dissolved in 7.5 M  $\text{HNO}_3$ , spiked with a mixed  $^{236}\text{U}/^{229}\text{Th}$  spike (for spike details see [14]) and heated to destroy organic material. The samples were centrifuged and the small undissolved detrital portion removed. U and Th were separated from the soluble fraction using a modified version of the chemistry described in Edwards et al. [4]. U and Th concentrations and isotope ratios were measured by TIMS and multiple collector inductively coupled plasma mass spectrometry (MC–ICP–MS). Techniques for TIMS analyses are based on those of Edwards et al. [4] and are fully detailed in Henderson et al. [14]. MC–ICP–MS analysis of U and Th has previously been demonstrated [15,16]. In this study, such analyses were performed by aspirating U and Th through a Cetac Aridus nebuliser into a Nu MC–ICP–MS, which provides ion yields for both elements of  $\sim 1\%$ . Full details for the MC–ICP–MS analysis are given below.

U was measured statically with  $^{238}\text{U}$ ,  $^{236}\text{U}$ , and  $^{235}\text{U}$  in Faraday collectors, and  $^{234}\text{U}$  in an ion-counting channel that has an abundance sensitivity of better than 5 ppm at 1 amu. This causes an offset to the measured  $^{235}\text{U}/^{234}\text{U}$  ratio of  $<0.5\%$  that is almost entirely corrected by the standard-bracketing measurement protocol described below. Forty-five 10-s integrations were collected for each sample at a  $^{234}\text{U}$  intensity of  $\sim 15 \times 10^3$  cps and a  $^{238}\text{U}$  beam of  $\sim 4$  V (with  $10^{11} \Omega$  resistors). Measured  $^{238}\text{U}/^{235}\text{U}$  was compared to its true value of 137.88 to correct for mass discrimination. Mass discrimination was very stable during a single day, and from day to day, at 7–8% per amu. Two replicate CRM-145 standards (formerly U-960) were analysed either side of each sample at similar intensities. The first of these standards was used to correct for ion-counter gain and drift in the sample and second standard. Ion-counter gain was close to 90% and remained stable during a day's analysis so that drift correction made little or no improvement to external reproducibility. The second standard allowed this external reproducibility to be assessed. The external reproducibility on the  $^{235}\text{U}/^{234}\text{U}$  was

1.3‰ (2S.D.,  $n = 39$ ) when measured over 3 days. This external reproducibility is 1.6 times the average internal error, and 1.9 times the expected counting statistics.

This measurement protocol returned identical values for CRM-145 over a range of  $^{238}\text{U}$  intensities from 1 to 9 V indicating that the ion-counting system behaves linearly. In practice, samples and standards were run in a narrow range of  $^{238}\text{U}$  intensities of 3–5 V. This intensity range ensures rapid collection of a large number of  $^{234}\text{U}$  ions, but does not allow for an internal assessment of ion-counter gain within run as the  $^{235}\text{U}$  beam is too large to collect in the ion-counter. The standard-bracketing approach was tested against lower concentration standards with the  $^{235}\text{U}$  in the ion-counter and yielded identical results. This consistency reflects the steadiness of the ion-counter gain.

Electronic backgrounds were measured before each analysis by switching both the electrostatic analyser and the magnet. Memory was assessed by monitoring all U beams between runs. U intensities dropped to 0.1‰ of their in-run value within 2 minutes of clean 2%  $\text{HNO}_3$  uptake. During analysis, wash times of 3 min were used between samples and standards. This protocol leads to a total collection time including washes, backgrounds and all sample switching, of 13 min for each standard or sample.

An assessment of the accuracy of the U analyses was performed by comparison of CRM-145 with the HU-1 secular-equilibrium standard. HU-1 was measured in place of the sample in the above protocol. The offset in  $\delta^{234}\text{U}$  values between HU-1 and CRM-145 was measured as  $-36.7 (\pm 1.7 \text{ 2S.D.}; n = 8)$ , identical to the best TIMS analyses [19] (Fig. 2).

Th isotopes were analysed multi-dynamically with  $^{230}\text{Th}$  and  $^{229}\text{Th}$  alternately in the same ion-counter and  $^{232}\text{Th}$  in a Faraday collector during each step. The lower dynamic range required for Th samples in this study than for U samples enables higher count rates on  $^{230}\text{Th}$  than on  $^{234}\text{U}$ . Beam intensities were approximately  $50 \times 10^3$  cps and 0.8 V for  $^{230}\text{Th}$  and  $^{232}\text{Th}$ , respectively. Twenty-five cycles with 10 s for each step were collected, leading to a total uptake of approxi-

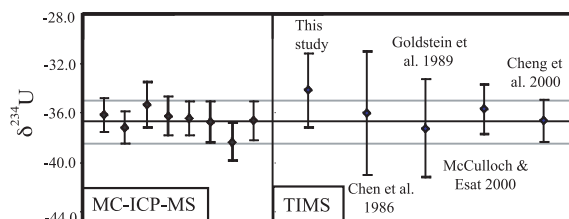


Fig. 2. Eight measurements of CRM-145 (formerly U960) relative to HU-1 on the Nu plasma MC-ICP-MS during a single day (see text for full analytical details). The mean difference in  $\delta^{234}\text{U}$  between these two standards was measured at  $-36.7 \pm 1.7\%$  (2S.D.) and is shown by the horizontal lines. These values are compared with TIMS measurements shown by crosses from five laboratories including the TIMS measurements of this study [19,41–43].

mately 250 ng of  $^{232}\text{Th}$ . The standard-bracketing approach described above for U was used. In the absence of appropriate certified standards, we used an in-house isotope standard, ‘ABC2’, which has isotope ratios similar to spiked average Bahamas carbonate ( $^{232}\text{Th}/^{230}\text{Th} = 718.06$ ,  $^{232}\text{Th}/^{229}\text{Th} = 399.11$ , and  $^{230}\text{Th}/^{229}\text{Th} = 0.55589$ ). External 2S.D. reproducibility on this standard was better than 1‰ for all three isotope ratios and was, again, 1.6 times the internal error and 1.9 times the expected counting statistics. This level of precision on  $^{230}\text{Th}/^{229}\text{Th}$  analyses is a considerable improvement over that achieved by most TIMS techniques, particularly on these Bahamas samples where the reasonably large  $^{232}\text{Th}$  contents tend to reduce thermal ionisation efficiency.

There are two methods to correct for mass discrimination in thorium samples. The first is to assume that it was identical to that measured in bracketing standards, the second is to make use of the incomplete U–Th separation during chemistry and to monitor the  $^{238}\text{U}/^{235}\text{U}$  within run. Both approaches were used and yield identical results at the 1‰ level.

Th memory is more persistent than that of U. Wash times of 4 min were used after which time the  $^{232}\text{Th}$  beam had reduced to 1‰ of its in-run value. To minimise the effect of memory, samples and standards were run at similar  $^{232}\text{Th}$  intensities, and the standard has a similar isotope ratio to the samples analysed. Washing with 10% and then 2%  $\text{HNO}_3$  repeatedly can reduce Th memory further, but this approach was not required here.

Table 1  
TIMS and MC-ICP-MS data from Cores 1008 and 1009

Depth (mbsf)	<sup>238</sup> U (ppm)	<sup>230</sup> Th (ppt)	( <sup>232</sup> Th/ <sup>230</sup> Th)	δ <sup>234</sup> U(O) (‰)	( <sup>230</sup> Th/ <sup>238</sup> U)	Age <sub>raw</sub> (ka)	Detrital (%)	Age <sub>corr</sub> (ka)	δ <sup>234</sup> U(T) <sub>corr</sub> (‰)
1008									
TIMS:									
12.48	7.60 ± 0.02	109.74 ± 0.68	164.30 ± 1.23	105.17 ± 2.52	0.883 ± 0.006	167.0 ± 2.73	0.64	163.30 ± 3.30	166.88 ± 3.70
13.48	8.13 ± 0.02	51.04 ± 0.55	55.75 ± 0.79	96.38 ± 3.15	0.384 ± 0.004	46.72 ± 0.66	0.56	38.64 ± 4.09	107.47 ± 4.57
<b>14.98</b>	<b>6.20 ± 0.02</b>	<b>102.29 ± 0.87</b>	<b>187.13 ± 0.81</b>	<b>93.29 ± 2.78</b>	<b>0.903 ± 0.004</b>	<b>181.53 ± 2.38</b>	<b>0.49</b>	<b>178.41 ± 2.84</b>	<b>155.11 ± 4.35</b>
<b>15.48</b>	<b>8.26 ± 0.02</b>	<b>106.94 ± 0.58</b>	<b>200.33 ± 1.69</b>	<b>88.04 ± 2.54</b>	<b>0.911 ± 0.007</b>	<b>188.51 ± 3.87</b>	<b>0.49</b>	<b>184.72 ± 4.31</b>	<b>148.39 ± 4.09</b>
17.98	3.61 ± 0.01	56.67 ± 0.70	53.02 ± 0.83	94.44 ± 3.47	0.959 ± 0.012	213.08 ± 8.57	0.95	200.77 ± 10.55	169.21 ± 4.70
18.48	5.16 ± 0.01	63.80 ± 0.51	118.00 ± 1.38	87.30 ± 2.16	0.961 ± 0.009	219.34 ± 6.92	0.71	215.09 ± 7.23	161.19 ± 5.32
<b>19.48</b>	<b>4.04 ± 0.01</b>	<b>91.52 ± 0.34</b>	<b>137.62 ± 1.39</b>	<b>78.86 ± 2.31</b>	<b>0.964 ± 0.008</b>	<b>228.77 ± 6.64</b>	<b>0.49</b>	<b>225.32 ± 6.86</b>	<b>150.40 ± 4.64</b>
19.98	2.85 ± 0.01	123.08 ± 0.87	32.76 ± 0.32	103.35 ± 2.75	0.994 ± 0.008	230.93 ± 6.58	1.13	209.62 ± 12.52	190.97 ± 3.76
MC-ICP-MS:									
<b>0.10</b>	<b>3.92 ± 0.01</b>	<b>5.23 ± 0.03</b>	<b>12.98 ± 0.08</b>	<b>146.71 ± 1.12</b>	<b>0.082 ± 0.001</b>	<b>8.05 ± 0.05</b>	<b>0.35</b>	<b>2.25 ± 2.90</b>	<b>148.25 ± 1.47</b>
<b>5.12</b>	<b>4.92 ± 0.01</b>	<b>14.41 ± 0.05</b>	<b>23.02 ± 0.06</b>	<b>144.38 ± 0.71</b>	<b>0.179 ± 0.001</b>	<b>18.51 ± 0.08</b>	<b>0.54</b>	<b>11.38 ± 3.56</b>	<b>149.69 ± 1.43</b>
<b>8.70</b>	<b>7.21 ± 0.02</b>	<b>89.94 ± 0.16</b>	<b>153.74 ± 0.10</b>	<b>100.52 ± 1.09</b>	<b>0.762 ± 0.002</b>	<b>125.13 ± 0.75</b>	<b>0.62</b>	<b>121.79 ± 1.85</b>	<b>142.57 ± 1.59</b>
11.98	9.33 ± 0.02	112.28 ± 0.20	56.78 ± 0.04	98.24 ± 0.96	0.736 ± 0.002	118.04 ± 0.58	1.59	106.28 ± 5.93	133.53 ± 2.27
<b>12.99</b>	<b>7.33 ± 0.02</b>	<b>107.39 ± 0.19</b>	<b>156.63 ± 0.10</b>	<b>81.92 ± 0.87</b>	<b>0.896 ± 0.002</b>	<b>183.84 ± 1.30</b>	<b>0.62</b>	<b>179.58 ± 2.50</b>	<b>136.34 ± 1.62</b>
15.86	7.67 ± 0.02	114.85 ± 0.22	261.32 ± 0.18	77.43 ± 1.04	0.915 ± 0.002	197.05 ± 1.58	0.46	195.01 ± 1.88	134.54 ± 1.83
<b>16.49</b>	<b>6.93 ± 0.02</b>	<b>103.73 ± 0.19</b>	<b>197.60 ± 0.13</b>	<b>78.13 ± 0.71</b>	<b>0.914 ± 0.002</b>	<b>196.06 ± 1.46</b>	<b>0.53</b>	<b>193.25 ± 2.03</b>	<b>135.11 ± 1.30</b>
<b>16.98</b>	<b>5.79 ± 0.01</b>	<b>86.92 ± 0.16</b>	<b>134.60 ± 0.09</b>	<b>78.64 ± 0.91</b>	<b>0.917 ± 0.002</b>	<b>197.24 ± 1.53</b>	<b>0.58</b>	<b>192.28 ± 2.91</b>	<b>135.87 ± 1.74</b>
<b>17.49</b>	<b>4.49 ± 0.01</b>	<b>69.30 ± 0.13</b>	<b>82.04 ± 0.06</b>	<b>78.91 ± 1.19</b>	<b>0.942 ± 0.003</b>	<b>212.89 ± 1.91</b>	<b>0.59</b>	<b>202.45 ± 5.56</b>	<b>140.56 ± 2.78</b>
<b>17.98</b>	<b>5.37 ± 0.01</b>	<b>84.44 ± 0.17</b>	<b>210.89 ± 0.16</b>	<b>75.95 ± 0.88</b>	<b>0.961 ± 0.003</b>	<b>228.58 ± 2.22</b>	<b>0.29</b>	<b>224.54 ± 3.00</b>	<b>143.69 ± 1.80</b>
<b>18.48</b>	<b>5.16 ± 0.01</b>	<b>80.79 ± 0.14</b>	<b>115.37 ± 0.09</b>	<b>77.06 ± 0.94</b>	<b>0.957 ± 0.002</b>	<b>224.94 ± 2.03</b>	<b>0.71</b>	<b>220.61 ± 2.97</b>	<b>144.6 ± 1.84</b>
<b>19.48</b>	<b>4.58 ± 0.01</b>	<b>72.11 ± 0.13</b>	<b>147.21 ± 0.13</b>	<b>69.89 ± 0.63</b>	<b>0.963 ± 0.003</b>	<b>235.77 ± 2.24</b>	<b>0.48</b>	<b>232.10 ± 2.90</b>	<b>135.42 ± 1.28</b>
20.98	8.49 ± 0.02	124.22 ± 0.21	180.52 ± 0.07	62.86 ± 0.77	0.894 ± 0.002	193.27 ± 1.42	0.59	189.20 ± 2.50	107.84 ± 1.39
24.49	8.80 ± 0.02	141.66 ± 0.25	416.13 ± 0.23	53.01 ± 0.67	0.983 ± 0.003	275.93 ± 3.35	0.40	275.70 ± 3.35	115.57 ± 1.46
1009									
TIMS:									
39.26	6.07 ± 0.02	58.17 ± 0.47	44.17 ± 0.48	109.48 ± 4.34	0.586 ± 0.005	80.65 ± 1.10	0.60	64.13 ± 8.35	132.77 ± 2.39
44.19	8.73 ± 0.02	126.09 ± 0.62	249.10 ± 1.42	105.76 ± 2.70	0.882 ± 0.005	166.66 ± 2.31	0.28	162.45 ± 3.15	168.56 ± 5.48
<b>46.19</b>	<b>7.99 ± 0.02</b>	<b>117.87 ± 1.36</b>	<b>316.59 ± 4.20</b>	<b>85.72 ± 4.34</b>	<b>0.901 ± 0.011</b>	<b>184.53 ± 6.04</b>	<b>0.35</b>	<b>182.23 ± 6.16</b>	<b>144.75 ± 7.32</b>
<b>48.18</b>	<b>12.10 ± 0.03</b>	<b>165.84 ± 0.87</b>	<b>863.28 ± 5.07</b>	<b>98.16 ± 2.54</b>	<b>0.837 ± 0.005</b>	<b>151.21 ± 1.99</b>	<b>0.18</b>	<b>150.28 ± 2.05</b>	<b>150.99 ± 4.33</b>
<b>52.69</b>	<b>5.09 ± 0.01</b>	<b>77.32 ± 0.80</b>	<b>436.71 ± 5.64</b>	<b>83.24 ± 2.83</b>	<b>0.929 ± 0.010</b>	<b>201.39 ± 6.31</b>	<b>0.28</b>	<b>200.98 ± 6.32</b>	<b>148.92 ± 5.08</b>
<b>56.35</b>	<b>9.42 ± 0.02</b>	<b>135.75 ± 0.69</b>	<b>333.40 ± 2.11</b>	<b>88.89 ± 2.68</b>	<b>0.881 ± 0.005</b>	<b>173.09 ± 2.58</b>	<b>0.21</b>	<b>169.61 ± 3.12</b>	<b>144.97 ± 3.90</b>
<b>57.68</b>	<b>5.01 ± 0.01</b>	<b>75.39 ± 0.72</b>	<b>197.72 ± 2.40</b>	<b>86.58 ± 4.85</b>	<b>0.919 ± 0.009</b>	<b>193.49 ± 5.90</b>	<b>0.42</b>	<b>190.69 ± 6.07</b>	<b>150.55 ± 8.40</b>
<b>60.20</b>	<b>4.45 ± 0.01</b>	<b>67.60 ± 1.62</b>	<b>344.19 ± 8.34</b>	<b>82.18 ± 2.68</b>	<b>0.929 ± 0.022</b>	<b>202.16 ± 14.55</b>	<b>0.18</b>	<b>199.36 ± 14.62</b>	<b>147.02 ± 4.43</b>
<b>63.18</b>	<b>5.66 ± 0.02</b>	<b>87.54 ± 0.99</b>	<b>154.03 ± 2.36</b>	<b>82.36 ± 8.81</b>	<b>0.945 ± 0.011</b>	<b>212.02 ± 10.03</b>	<b>0.60</b>	<b>208.35 ± 10.20</b>	<b>150.55 ± 16.05</b>
65.20	3.38 ± 0.01	52.79 ± 0.25	41.52 ± 0.79	83.82 ± 2.97	0.955 ± 0.005	218.01 ± 4.15	0.81	196.23 ± 11.69	149.81 ± 5.50
<b>66.69</b>	<b>6.29 ± 0.02</b>	<b>99.31 ± 1.43</b>	<b>329.07 ± 5.79</b>	<b>72.92 ± 4.38</b>	<b>0.964 ± 0.014</b>	<b>233.72 ± 12.70</b>	<b>0.35</b>	<b>232.11 ± 12.73</b>	<b>142.35 ± 8.51</b>
MC-ICP-MS:									
36.68	6.15 ± 0.02	77.82 ± 0.14	64.88 ± 0.05	102.48 ± 1.47	0.773 ± 0.002	128.20 ± 0.73	0.95	117.31 ± 5.51	144.30 ± 2.59
<b>43.19</b>	<b>8.14 ± 0.02</b>	<b>106.70 ± 0.19</b>	<b>143.97 ± 0.10</b>	<b>96.51 ± 0.93</b>	<b>0.801 ± 0.002</b>	<b>138.75 ± 0.77</b>	<b>0.54</b>	<b>133.21 ± 2.90</b>	<b>141.28 ± 1.60</b>
<b>55.68</b>	<b>5.17 ± 0.01</b>	<b>77.46 ± 0.14</b>	<b>354.01 ± 0.31</b>	<b>81.81 ± 0.88</b>	<b>0.915 ± 0.002</b>	<b>194.32 ± 1.49</b>	<b>0.16</b>	<b>191.55 ± 2.06</b>	<b>141.74 ± 1.52</b>
<b>56.35</b>	<b>5.63 ± 0.01</b>	<b>85.00 ± 0.16</b>	<b>342.04 ± 0.28</b>	<b>80.71 ± 0.90</b>	<b>0.923 ± 0.003</b>	<b>199.65 ± 1.61</b>	<b>0.20</b>	<b>197.13 ± 2.07</b>	<b>141.94 ± 1.59</b>
<b>56.68</b>	<b>5.45 ± 0.01</b>	<b>82.17 ± 0.16</b>	<b>311.79 ± 0.24</b>	<b>80.36 ± 1.21</b>	<b>0.922 ± 0.003</b>	<b>199.11 ± 1.69</b>	<b>0.20</b>	<b>196.12 ± 2.28</b>	<b>140.98 ± 2.13</b>
66.20	6.71 ± 0.02	105.60 ± 0.21	381.76 ± 0.41	67.11 ± 0.88	0.961 ± 0.003	237.08 ± 2.40	0.23	234.95 ± 2.64	131.05 ± 1.72
<b>66.69</b>	<b>6.51 ± 0.02</b>	<b>102.66 ± 0.23</b>	<b>332.67 ± 0.43</b>	<b>71.39 ± 0.97</b>	<b>0.963 ± 0.003</b>	<b>234.37 ± 2.50</b>	<b>0.24</b>	<b>231.69 ± 2.85</b>	<b>138.30 ± 1.88</b>
<b>70.69</b>	<b>6.49 ± 0.02</b>	<b>102.82 ± 0.19</b>	<b>202.04 ± 0.14</b>	<b>70.21 ± 1.06</b>	<b>0.968 ± 0.003</b>	<b>240.09 ± 2.51</b>	<b>0.38</b>	<b>235.90 ± 3.29</b>	<b>137.71 ± 2.14</b>

Depths are in metres below sea floor, round brackets denote activity ratio. U and Th blanks are < 1‰ of the measured sample and are corrected for. Raw ages and δ<sup>234</sup>U values are adjusted to account for initial <sup>230</sup>Th to give the corrected numbers in the final two columns. Errors are 2σ (except where labelled otherwise) and are propagated through the age calculation. All calculations have used the half-lives measured in Cheng et al. [19]. Samples with a δ<sup>234</sup>U(T)<sub>corr</sub> and (<sup>230</sup>Th/<sup>232</sup>Th) deemed acceptable are in bold.

Total analysis time for a Th sample or standard was 16 min. The enhanced precision and speed of U–Th analyses by MC-ICP-MS represents a significant step forward in our ability to analyse these isotope systems as has been shown in previous studies [15,16].

A 50 mg aliquot of each sample was diluted to 10 mg/ml after dissolution and analysed by inductively coupled atomic emission spectrometry (ICP-AES) to determine the concentration of Al and Ca. Al concentrations were used to estimate the abundance of detrital material in the dissolved sample. Oxygen isotope analysis was performed both on bulk sediment samples and on *G. sacculifer* (300–355 mm). A total of 165 *G. sacculifer* samples were measured on Core 1009 and 110 in Core 1008, with a resolution of 1–2 kyr during MIS 7.

#### 4. Results

Forty-one samples were analysed for U and Th, 22 from Core 1008 and 19 from Core 1009 (Table 1). Uranium concentrations range from 3 to 12 ppm with an average of 6.4 ppm.  $^{230}\text{Th}$  concentrations are as low as 5 ppt in Holocene samples and as high as 166 ppt in older samples. Holocene ( $^{230}\text{Th}/^{232}\text{Th}$ ) ratios are low, below 25 (rounded brackets denote activity ratios) reflecting the lack of time for  $^{230}\text{Th}$  ingrowth. Pre-Holocene samples have ratios from 33 to 863, with an average of 160 in Core 1008 and 290 in Core 1009. Only seven pre-Holocene samples have ( $^{230}\text{Th}/^{232}\text{Th}$ ) lower than 75. Raw ages are calculated from the ( $^{230}\text{Th}/^{238}\text{U}$ ) ratio and  $\delta^{234}\text{U}(0)$  (where  $\delta^{234}\text{U}(0) = \{((^{234}\text{U}/^{238}\text{U})_{\text{meas}}/(^{234}\text{U}/^{238}\text{U})_{\text{eq}}) - 1\} \times 10^3$ ) with half-lives following Cheng et al. [19]. Based on measured Al concentrations, the percentage of detrital material within the dissolved fraction ranges from 0.2 to 1.93 wt%, with average values of 0.6 wt% in Core 1008 and 0.4 wt% in Core 1009. Ages are corrected for initial  $^{230}\text{Th}$  based on assumptions about the  $^{230}\text{Th}$  in the detrital component (see Section 5.2 for full explanation). Corrections may be as large as 21 kyr, but the average is 5.3 kyr.  $\delta^{234}\text{U}(T) = \delta^{234}\text{U}(0)e^{-234\lambda t}$  (where  $t$  is the time of carbonate formation) range

from 107 to 191. More than 70% of the samples have values in the range 135–155. Four samples were replicated. Two of these replicates were in agreement with one another. In the second two cases the  $\delta^{234}\text{U}$  values were significantly different, suggesting that diagenetic processes in the sediment are very localised when they occur. The surprisingly young TIMS age of 170 ka at 56.35 m in Core 1009 was repeated by MC-ICP-MS and gave an age of 197 ka, suggesting that the first sample had been subject to confusion in the preparatory procedure.

#### 5. Discussion

##### 5.1. Stratigraphy

Throughout this study we denote marine isotope stages with a letter, e.g. MIS 7e. These substages refer to periods of time between events following Imbrie et al. [1]. The events themselves, corresponding to a point in time rather than a period, are denoted with a number, e.g. MIS 7.5, following Martinson et al. [2]. Glacial terminations are defined as the midpoint of the change in the  $\delta^{18}\text{O}$ .

The  $\delta^{18}\text{O}$  stratigraphy of Cores 1008 and 1009 clearly show the main glacial and interglacial stages that are recorded in deep-sea marine records (Fig. 3). Interglacial  $\delta^{18}\text{O}$  values are determined as strongly negative values that are distinct from the positive glacial values. Interglacial periods dominate the length of the core as high sea level causes the banks to flood and dramatically increases aragonite production and hence sedimentation rates. Glacial Terminations I to III are clearly seen marking the start of the Holocene, MIS 5 and MIS 7. Higher sample resolution during MIS 7 also reveals some internal features. The end of MIS 7e is defined by high  $\delta^{18}\text{O}$  values at 18.5 m below sea floor (mbsf) in Core 1008 and at  $\sim 65$  mbsf in Core 1009. Additionally, the sediment in Core 1009 is lithified at this depth as expected for periods of low sea level during MIS 7d. Other substages of MIS 7 are not clearly resolved, which is common even in deep-sea  $\delta^{18}\text{O}$  records where the MIS 7c–7a sequence tends to be

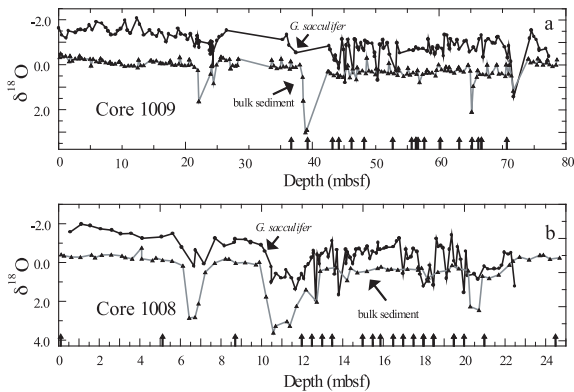


Fig. 3.  $\delta^{18}\text{O}$  stratigraphy of cores 1008 and 1009. New bulk sediment measurements are augmented by data in Malone et al. [44] and are consistent with the stratigraphy based on *G. sacculifer*. Grey lines are bulk sediment data and black lines are *G. sacculifer* data. Within MIS 7 substages 7e and 7d can be identified but other substages are not seen at this resolution. Arrows show the depths at which U-series dating was performed.

characterised by rather small  $\delta^{18}\text{O}$  changes. The end of MIS 7 is difficult to identify confidently in both cores. We tentatively place it at  $\sim 12.7$  mbsf in Core 1008 where both bulk and *G. sacculifer*  $\delta^{18}\text{O}$  show a sharp positive shift and  $\sim 50.5$  mbsf in Core 1009. This assignment would suggest that the low  $\delta^{18}\text{O}$  feature at  $\sim 12.1$  mbsf in Core 1008 represents a warm period within MIS 6.

MIS 5 is characterised in these cores by a single peak. This feature may reflect the lower sample resolution through this interval, although most Bahamas cores do not contain a distinctive MIS 5e–5a sequence. It is most likely that the single MIS 5 peak reflects the fact that the banks were only flooded once during this interval, probably during MIS 5e as in other records [13].

Termination III is marked by a large change of  $\delta^{18}\text{O}$  in bulk and *G. sacculifer* records in both cores, but in the deeper core large fluctuations in foraminiferal  $\delta^{18}\text{O}$  are associated with the termination. The termination is at 71.5 mbsf in Core 1009 and 20.2 mbsf in Core 1008. These fluctuations are probably due to the inclusion of glacial foraminifers mixed upwards in the sediment and occur in the deeper core because the sedimentation rate is slower. We place the beginning of MIS 7 in this core at the midpoint of the first change

from positive glacial values to negative interglacial  $\delta^{18}\text{O}$  values. The stage boundaries are based not only on  $\delta^{18}\text{O}$  but also on carbonate mineralogy, lithostratigraphy and nannofossil data [17].

Several lines of evidence indicate that down-slope transport during high-stands in these cores is not a problem. The reasonable  $^{14}\text{C}$  stratigraphy observed in the Holocene portion [12], for instance, argues against significant slumping events. Similarly, the consistent age versus depth relationship shown in this study suggests little down-slope transport. The  $\delta^{234}\text{U}(\text{T})$  values also indicate that most of the stratigraphy has not been subject to significant mixing. If the sediments are not mixed, or are mixed only with sediment of a similar age when washed down the slope,  $\delta^{234}\text{U}(\text{T})$  remains close to the seawater value. If, however, young and old material are mixed together then the resulting  $\delta^{234}\text{U}(\text{T})$  is somewhat lowered due to the different half-lives of  $^{234}\text{U}$  and  $^{230}\text{Th}$ . Therefore, the initial  $\delta^{234}\text{U}(\text{T})$  values observed in this study also suggest that the sediment is part of a coherent stratigraphy.

The main difference between these Bahamian records and those recorded in deep sediments is in the amplitude of the glacial to interglacial transition. If sea level alone were responsible for the shift in  $\delta^{18}\text{O}$  then we would expect to see a shift of approximately 1‰. In the Bahamas we see a range of up to 3‰ in both bulk and *G. sacculifer* records. Two ways to explain this difference might be a response to local sea surface temperature (SST) or a function of diagenesis during low-stand periods [17]. No direct data exist which constrain the timing of changes in SST in the Bahamas relative to the timing of global  $\delta^{18}\text{O}$  changes. The CLIMAP reconstruction of SST changes, however, did include cores from north and south of the Bahamas [20]. Across Termination II, and across other climate transitions studied in CLIMAP, no significant difference in the timing of SST and  $\delta^{18}\text{O}$  was observed and, if anything, SST lags  $\delta^{18}\text{O}$  very slightly. Unfortunately, the CLIMAP reconstructions do not extend to MIS 7, but from the data on younger periods it is probable that temperature and ice volume components of our  $\delta^{18}\text{O}$  records are synchronous at Termination III.

It is unlikely that the combination of temperature and ice volume changes together can explain the full 3‰ range of  $\delta^{18}\text{O}$  observed. These two factors alone would imply temperature changes of up to 9°C that are outside the range expected for low-latitude Pleistocene variability. It appears that some of the  $\delta^{18}\text{O}$  signal in these cores reflects seafloor diagenesis. Cementation on the seafloor is known to occur in the Bahamas environment when sedimentation rates are low [17,18]. During sea-level low-stands when the banks are exposed, the lower sedimentation rates lead to calcite cementation. As this cement is formed in waters that are somewhat colder than the surface waters, they have a higher  $\delta^{18}\text{O}$ . This contribution to the signal amplifies the high  $\delta^{18}\text{O}$  values expected for cold glacial periods. The range of  $\delta^{18}\text{O}$  seen in the ODP Leg 166 cores is larger than that seen in cores taken from the flanks of the Little Bahama Bank where smaller variability in sedimentation rates give rise to lower cementation rates. Any component of  $\delta^{18}\text{O}$  variability in Bahamas cores attributable to this diagenesis is expected to be directly related to the sea level. This diagenesis is not expected to perturb the U–Th system for two reasons. Firstly, it happens at the seafloor and therefore is synchronous with sediment formation. Secondly, inorganic carbonate precipitates contain rather low U concentrations compared with the high U contents of the biogenic aragonite material in these sediments.

In summary, the large 3‰ range in  $\delta^{18}\text{O}$  observed in these cores reflects a combination of global ice volume, local temperature, and seafloor diagenesis during glacials. These three effects are expected to vary synchronously in the Bahamas environment at glacial terminations so that dating of the  $\delta^{18}\text{O}$  records in these cores is expected to provide age information for the history of global ice volume. Phasing between sea level and temperature is less well constrained during the transition out of interglacial conditions, so these portions of our records are somewhat harder to interpret.

### 5.2. Age correction

In order to use the ingrowth of  $^{230}\text{Th}$  as a chronometer we must either assume that its initial

concentration was zero, or estimate an initial concentration to correct the measured age. Corals have proved successful for U-series dating in part since their initial  $^{230}\text{Th}$  concentration is negligible. However, the presence of  $^{232}\text{Th}$  in Bahamian sediments indicates that a proportion of the  $^{230}\text{Th}$  is primary rather than a product of ingrowth. We correct for this initial thorium following the approach of Slowey et al. [13]. This correction technique is appropriate for interglacial sediments with a low initial thorium content. In cases where initial thorium is more significant, for instance during glacial periods, then it is more appropriate to use an isochron technique [7]. The Al concentration of the sediment is used as a proxy for dust content in order to estimate how much Th is associated with detritus. Any  $^{232}\text{Th}$  not accounted for by this detritus must be derived from seawater by scavenging.

We assume that the detrital material has an Al concentration of 15 wt%, a U content of 2.8 ppm, and a Th content of 10 ppm. These values represent typical crustal concentrations [21] and we assume that the U-series nuclides are at secular equilibrium. We assume a seawater ( $^{230}\text{Th}/^{232}\text{Th}$ ) of 18 [13]. Since the composition of the detritus and the Th-isotope ratio of seawater are not precisely known, the error on the correction is substantial and we estimate it conservatively at  $\pm 50\%$ . This level of uncertainty in the correction represents a significant portion of the final error on TIMS ages and totally dominates the final error for MC–ICP–MS ages. Where the age correction is large, the ages are discarded as the resulting errors render them of little use. Samples are therefore rejected if their ( $^{230}\text{Th}/^{232}\text{Th}$ ) is less than 75, representing a typical age correction of  $\sim 10$  kyr, and an associated error of  $> 5$  kyr. Exceptions are made of the two Holocene samples in Core 1008 because here it is the low value of ingrown  $^{230}\text{Th}$  that causes the ( $^{230}\text{Th}/^{232}\text{Th}$ ) ratio to be small.

### 5.3. Diagenesis

Ages measured in this study generally increase with stratigraphic depth as expected. However, a few samples are clearly no longer pristine.  $\delta^{234}\text{U}$  is

commonly used to assess the extent of diagenesis in corals from terraces [4]. Seawater  $\delta^{234}\text{U}$  is thought to be close to its present value at MIS 7 [10,22,26]. If the Bahamian sediments have remained a closed system then they should have a  $\delta^{234}\text{U}(\text{T})$  close to the modern day value of  $145.8 \pm 1.7\text{‰}$  [19]. Measured  $\delta^{234}\text{U}(\text{T})$  in the sediments are generally near to 145.8 suggesting that they have been a closed system. Twelve of the 41 samples in this study lie outside the range 135–155 and are considered to be unreliable, as the U–Th system has clearly been affected. Altered samples generally lie close to low-stand periods of slow sedimentation when reworking, mixing or diagenesis are more likely to have occurred.

#### 5.4. U–Th ages

Twenty-seven of the 41 samples analysed pass the two isotope criteria set out above and these produce a consistent chronology for each core. U–Th ages from the Holocene and MIS 5 in Core 1008 confirm that the stratigraphic sequence is substantially complete. Samples from the top and bottom of the Holocene return ages of 2 and 11 ka as expected, and the one MIS 5e age is 122 ka. Twenty-one samples with reliable ages fall within the low  $\delta^{18}\text{O}$  values interpreted as MIS 7. These ages approximately double the number of reliable ages available for MIS 7. Reliable ages range from 232 to 178 ka in Core 1008 and from 236 to 191 ka in Core 1009. We see an age reversal in the youngest part of MIS 7 in core 1009 suggesting a repeated section of sediment. As  $\delta^{234}\text{U}(\text{T})$  is within the accepted range it is more likely that this section moved as a coherent unit rather than experiencing mixing.

#### 5.5. Comparison of new ages to other MIS 7 ages

##### 5.5.1. Existing constraints for MIS 7

Orbitally tuned timescales such as SPECMAP suggest that MIS 7 lasted from  $\sim 245\text{--}190$  ka [1]. Within this time range there are very few published U–Th dates that have both reliable  $\delta^{234}\text{U}(\text{T})$  values and a realistic palaeo sea-level estimate. Uncertainties in sea-level reconstructions for corals arise from two areas; an expected depth

range of the living coral, and subsequent tectonic motion. The coral *Acropora palmata* is frequently sampled, and is assumed to live within 5 m of the surface. Although this is the common range, some modern day examples live as deep as 20 m [23]. Vertical tectonic movement is usually calculated by linear extrapolation of the age and height of MIS 5e terraces, assuming that sea level was then at 5 m. A realistic estimate of the uncertainty, based on the common depth range of *A. palmata*, is  $-15/+10$  m. In cases where the sample comes from a beach deposit the problem of the variable depth range of the live coral is negated [10,24] and the sea-level estimate is more precise. Coral reefs can provide excellent records for interglacials in tectonically stable areas, where there has been little diagenesis and where we can be certain of the depth of growth/deposition. However these conditions are rarely met in corals as old as MIS 7 and it can still be difficult to ascribe these samples to particular portions of the MIS curve.

In the literature, five corals from Barbados are the only MIS 7 samples with  $\delta^{234}\text{U}(\text{T})$  indicative of a closed U–Th system. Barbados is tectonically uplifting at a rate of 0.11–0.45 m/kyr [25]. This uplift rate has large uncertainties as the island is tilted, with high rates on the western coast and much lower rates on the south and east coasts. One coral (WAN-B-2) is at a present elevation of 91 m and has yielded ages with good  $\delta^{234}\text{U}(\text{T})$  ranging from 190.2 to 201.2 ka (five replicates give 190.2, 191.7, 193.1, 199.0, 201.2 ka) [10,24]. These ages are not within error of each other so they cannot be considered reliable. A second coral (WAN-B7) at 91 m yielded an age of  $200.8 \pm 1.0$  [10,24], with a suggested sea level of  $-3$  to  $+8$  m relative to present sea level (mrpsl). A third coral (WAN-B-1) from 91 m has a single age of  $193.5 \pm 2.8$  ka [10] and an initial elevation of 0 to  $+11$  mrpsl (Gallup, 2001, personal communication). The fourth coral at a present day elevation of 40 m has an age of  $187 \pm 6$  ka and an estimated palaeo sea level of 2.6 mrpsl [26]. A final coral with concordant Pa and U–Th ages and with an acceptable  $\delta^{234}\text{U}$  has an age of  $168.0 \pm 1.3$  ka and an initial sea level of  $-38$  mrpsl [8]. The constraints on sea level from these corals are shown on Fig. 5.

In contrast to corals, speleothems form when subaerially exposed, providing information on the timing of low-stands. A hiatus is usually interpreted as a time during which the sample was submerged, or when climatic conditions (e.g. low rainfall), precluded further growth. Therefore constraints on the timing of high-stands are between dated periods of continuous growth in speleothems. U-series dating is possible as the calcite incorporates U and virtually excludes Th. Reliability is difficult to assess geochemically as the history of groundwater  $\delta^{234}\text{U}$  is not constrained. However, speleothems are generally thought to be resistant to the effects of diagenesis because of a lack of pore spaces by which secondary water could infiltrate.

Four studies have used TIMS to date MIS 7 speleothems from Bahamian Blue Holes (submerged caves). On Grand Bahama Island two studies provide a suite of dates through MIS 7. Li et al. [27] quote ages from  $-10$  mrpsl which put high-stands at  $>280$ , 235–230 and 220–212 ka. Lundberg et al. [28] report consistent results from the same speleothem, although age errors are frequently in excess of 15 kyr. Speleothems from Andros Island have yielded more scattered ages. Richards et al. [29] report a single date at  $190 \pm 5$  ka from  $-15$  mrpsl. Smart et al. [30] used  $\alpha$  counting and TIMS to date samples from a greater range of depths. Age constraints on sea level are also determined from a speleothem in a submerged cave in Italy [31] This deposit suggests that the sea level was lower than  $-18.5$  mrpsl before 202 ka and after 190 ka. Speleothem data are summarised on Fig. 5.

### 5.5.2. The beginning of MIS 7

Extrapolation of the new MIS 7e ages in Core 1009 suggest that the full interglacial conditions of MIS 7 began at  $\sim 237$  ka. This age assumes that the sedimentation rate during MIS 7e is constant (Figs. 4 and 5). Core 1008 is less well constrained, but is consistent with this initiation for the peak of MIS 7. This timing is in good agreement with the only existing radiometric constraints from speleothems (Fig. 5). Allowing for a  $\sim 6$  kyr deglaciation as preserved in marine  $\delta^{18}\text{O}$  records [32] suggests a timing for Termina-

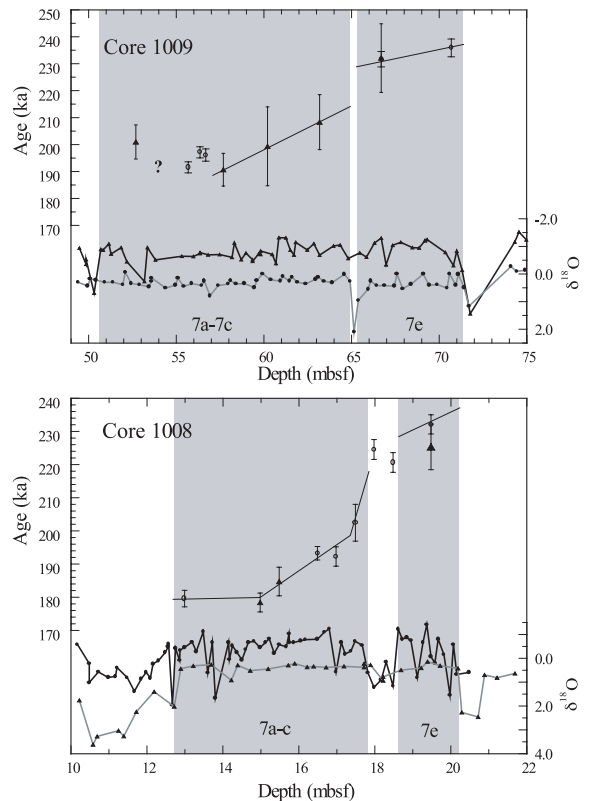


Fig. 4. These sections show enlarged MIS 7 stratigraphies together with reliable U-series ages, both from TIMS (solid triangles) and MC-ICP-MS (open circles). Age errors are  $2\sigma$  and include uncertainty due to correction for initial  $^{230}\text{Th}$  and analytical error. Black lines through ages suggest sedimentation rates through each substage. Grey shading indicates high-stand periods as labelled, selected on the basis of  $\delta^{18}\text{O}$  data.

tion III of  $\sim 240$  ka. This age is  $\sim 5$  kyr later than traditional orbitally tuned timescales [1,2] which place Termination III at  $\sim 245$  ka and is  $\sim 12$  kyr later than a new tuned record [33]. It is possible that sedimentation rates in our cores were lower in the very earliest portions of the peak of MIS 7 so the 240 ka age for Termination III may need to be increased somewhat. On the basis of work on MIS 5e and Termination II [13,14], any such increase would be expected to be only of order 2–3 kyr. This analysis therefore suggests that the benthic record of Karner et al. [33] is not correct for this interval. It also suggests

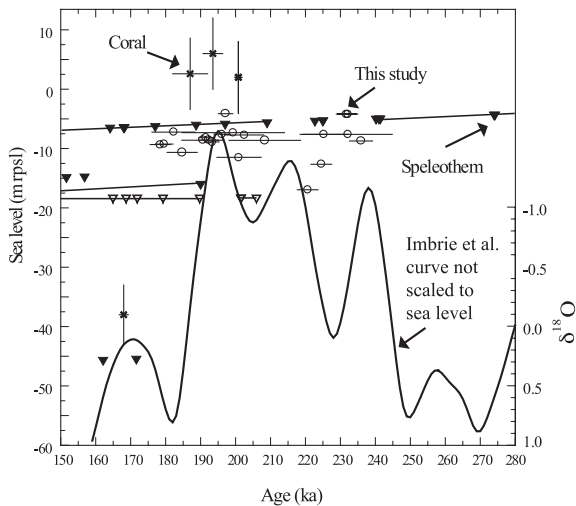


Fig. 5. Summary of radiometrically dated carbonates in the range 280–150 ka shown with the SPECMAP curve of Imbrie et al. [1] for comparison. Coral data from Barbados are shown as crosses with associated age and sea-level uncertainties [8,10,24,26]. Speleothem ages [27–30] from the Bahamas plotted as solid triangles show sea-level estimates plotted along a slope representing 0.02 m/kyr of subsidence, the maximum estimated value over 25 Myr [27]. Open triangles represent sea-level constraints from an Italian speleothem [31]. Solid lines between symbols represent periods of continuous growth. Speleothem ages with errors greater than 12 ka are excluded. Ages from this study are assigned a sea level based on the relative  $\delta^{18}\text{O}$  isotopic signature. This method is only intended to give an approximate indication of sea level for plotting purposes and does not imply precise sea level.

that the true timing of Termination III is either close to the SPECMAP chronology, or lags it by a few thousand years. This timing is in contrast to radiometric dating of Termination II which indicate that tuned chronologies place the termination too late by up to 8 kyr [7,8]. Termination III appears to be more like Termination I for which radiometric dates [34] are in good agreement with orbitally tuned records [1,2]. It seems that each termination reflects a differing response to orbital forcing.

### 5.5.3. MIS 7 substages

The 7e/7d transition is seen clearly in the *G. sacculifer* record of Core 1008. It is less distinct in Core 1009, but an obvious drop in sedimenta-

tion rate at the same time as a sharp peak in bulk  $\delta^{18}\text{O}$  in Core 1009 indicates the position of 7.4. Extrapolation of Core 1009 ages through 7e suggests that it lasts from 237 to 228 ka and, although less well constrained, Core 1008 is consistent with this timing. The beginning of the second interstadial, MIS 7.3, lies at  $\sim 215$  ka in both cores. The younger substages 7c–7a are not clearly defined, which is normal for marine  $\delta^{18}\text{O}$  records (e.g. [35]). The sedimentation rate changes during 7c–7a in Core 1008 because the low rate of sedimentation during stadial 7b has not been distinguished from the faster rates during the two interstadials.

### 5.5.4. The end of MIS 7

The end of MIS 7 in our records is complex and appears to occur up to 10 ka later than orbitally tuned timescales. Ages as young as 178.4 ka have interglacial  $\delta^{18}\text{O}$  values, whereas orbitally tuned timescales and coral/speleothem data suggest that MIS 7 ended at  $\sim 190$  ka. U and Th isotope criteria indicate reliable ages and the two cores give consistent chronologies throughout the rest of MIS 7 suggesting that this is not a dating problem. Sedimentary repetition of a portion of the high-stand sediment, as indicated by an age reversal in Core 1009, would also not explain these young ages for interglacial  $\delta^{18}\text{O}$  values. Speleothem dates from the Bahamas and Italy strongly suggest that sea level was falling rapidly around 190 ka [29,31]. Coral dates tend to agree, as there are no reliable high-stand coral ages younger than 187 ka [10,24,26]. If sea level did indeed fall at 190 ka and the Bahamian records still retain negative  $\delta^{18}\text{O}$  signals then there must be another important influence on the isotopes. A new speleothem record from Oman, also a low latitude locality, indicates that the end of MIS 7 was complex [36], and that interglacial conditions may have prevailed until  $\sim 180$  ka. We suggest that continued negative  $\delta^{18}\text{O}$  values in the Bahamas reflect continuing high temperature. The end of MIS 7 is clearly an enigmatic time. Further dating and stratigraphic work (e.g. palaeo-thermometry) may help to better understand this transition from interglacial to glacial conditions.

## 6. Summary

These Bahamian cores enable us to directly date a  $\delta^{18}\text{O}$  stratigraphy. Holocene and MIS 5 U–Th ages are as expected, showing that the stratigraphy reflects global climate change and that the sediments are highly suited for U–Th chronology. Using the high precision of MC-ICP-MS, we have more than doubled the number of reliable U–Th dates for MIS 7. These dates indicate that MIS 7 probably did not start any earlier than suggested by orbitally tuned records with the peak of MIS 7e lasting from approximately 237 to 228 ka. These ages are in agreement with published low precision speleothem ages [27,28]. MIS 7c is assessed to start at  $\sim 215$  ka. Later substages are not defined and the end of the MIS 7 is complex, with interglacial  $\delta^{18}\text{O}$  values lasting until  $\sim 180$  ka, possibly reflecting continued high temperatures in the area.

## Acknowledgements

We thank Nick Belshaw for his invaluable help and advice with MC-ICP-MS measurements. We are grateful to three careful reviews from Dr. Bard, Dr. Gallup and Dr. Stirling that significantly improved the text. This research was supported by the NERC by Grant No. GR3/12828; by NERC research studentship GT/04/99/ES/208 to L.F.R.; and by use of the ICP-AES facility at the Royal Holloway University of London. [AH]

## References

- [1] J. Imbrie, J.D. Hays, D.G. Martinson, A. McIntyre, A.C. Mix, J.J. Morley, N.G. Pisias, W.L. Pressl, N.J. Shackleton, The orbital theory of Pleistocene climate: support from a revised chronology of the marine  $\delta^{18}\text{O}$  record, in: A.L. Berger, J. Imbrie, J. Hays, G. Kukla, B. Salzman (Eds.), *Milankovitch and Climate*, Proc. NATO Workshop 1, NATO ASI Series C 126, Reidel, 1984, pp. 269–305.
- [2] D.G. Martinson, N.G. Pisias, J.D. Hays, J. Imbrie, T.C. Moore Jr., N.J. Shackleton, Age dating and the orbital theory of the ice ages development of a high-resolution 0 to 300000-year chronostratigraphy, *Quat. Res.* 27 (1987) 1–29.
- [3] M. Milankovitch, The influence of axial tilt and precession as the cause of glacial cycles, in: B. Gutenberg (Ed.), *Handbuch der Geophysik*, vol. 9, 1938, pp. 593–698.
- [4] R.L. Edwards, J.H. Chen, G.J. Wasserburg,  $^{238}\text{U}$ – $^{234}\text{U}$ – $^{230}\text{Th}$ – $^{232}\text{Th}$  systematics and the precise measurement of time over the past 500000 years, *Earth Planet. Sci. Lett.* 81 (1986) 175–192.
- [5] E. Bard, B. Hamelin, R.G. Fairbanks, U–Th ages obtained by mass spectrometry in corals from Barbados sea level during the past 130000 years, *Nature* 346 (1990) 456–458.
- [6] C.H. Stirling, T.M. Esat, M.T. McCulloch, K. Lambeck, High-precision U-series dating of corals from Western Australia and implications for the timing and duration of the last interglacial, *Earth Planet. Sci. Lett.* 135 (1995) 115–130.
- [7] G.M. Henderson, N.C. Slowey, Evidence from U–Th dating against Northern Hemisphere forcing of the penultimate deglaciation, *Nature* 404 (2000) 61–65.
- [8] C.D. Gallup, H. Cheng, D.W. Taylor, R.L. Edwards, Direct determination of the timing of sea level change during Termination II, *Science* (2002) in press.
- [9] F.C. Bassinot, L.D. Labeyrie, E. Vincent, X. Quidelleur, N.J. Shackleton, Y. Lancelot, The astronomical theory of climate and the age of the Brunhes-Matuyama magnetic reversal, *Earth Planet. Sci. Lett.* 126 (1994) 91–108.
- [10] C.D. Gallup, R.L. Edwards, R.G. Johnson, The timing of high sea levels over the past 200000 years, *Science* 263 (1994) 796–800.
- [11] G.P. Eberli, P.K. Swart, M.J. Malone, Sites 1008/1009, in: *Proc. Ocean Drilling Program, Initial Reports* 166, Bahamas transect, 1996, pp. 347–373.
- [12] N.C. Slowey, R.J. Wilbur, G.A. Haddad, G.M. Henderson, Glacial-to-Holocene sedimentation on the western slope of the Great Bahama Bank, *Mar. Geol.* (2002) in press.
- [13] N.C. Slowey, G.M. Henderson, W.B. Curry, Direct U–Th dating of marine sediments from the two most recent interglacial periods, *Nature* 383 (1996) 242–244.
- [14] G.M. Henderson, N.C. Slowey, M.Q. Fleisher, U–Th dating of carbonate platform and slope sediments, *Geochim. Cosmochim. Acta* 65 (2001) 2757–2770.
- [15] X. Luo, M. Rehkemper, L. Der-Chee, A.N. Halliday, High precision  $^{230}\text{Th}/^{232}\text{Th}$  and  $^{234}\text{U}/^{238}\text{U}$  measurements using energy filtered ICP magnetic sector multiple collector mass spectrometry, *Int. J. Mass Spectrom. Ion Process.* 171 (1997) 105–117.
- [16] C.H. Stirling, T.M. Esat, K. Lambeck, M.T. McCulloch, S.G. Blake, D.C. Lee, A.N. Halliday, Orbital forcing of the marine isotope stage 9 interglacial, *Science* 291 (2001) 290–293.
- [17] J.J. Malone, N.C. Slowey, G.M. Henderson, Early diagenesis of shallow-water peri-platform carbonate sediments, leeward margin, Great Bahama Bank (ODP Leg 166), *GSA Bull.* 113 (2001) 881–894.
- [18] N.C. Slowey, A.C. Neumann, K.C. Baldwin, Seismic expression of Quaternary climatic cycles in the peri-platform

- carbonate ooze of the northern Bahamas, *GSA Bull.* 101 (1989) 1563–1573.
- [19] H. Cheng, R.L. Edwards, J. Hoff, C.D. Gallup, D.A. Richards, Y. Asmeron, The half-lives of  $^{234}\text{U}$  and  $^{230}\text{Th}$ , *Chem. Geol.* 169 (2000) 17–33.
- [20] CLIMAP Project Members, The last interglacial ocean, *Quat. Res.* 21 (1984) 123–224.
- [21] S.R. Taylor, S.M. McLennan, *The Continental Crust: its Composition and Evolution*, Blackwell Scientific, Oxford, 1985.
- [22] G.M. Henderson, A.S. Cohen, R.K. O’Nions,  $^{234}\text{U}/^{238}\text{U}$  ratios and  $^{230}\text{Th}$  ages for Hateruma Atoll corals: implications for coral diagenesis and seawater  $^{234}\text{U}/^{238}\text{U}$  ratios, *Earth Planet. Sci. Lett.* 115 (1993) 65–73.
- [23] P. Humann, *Reef Coral Identification*, New World Publications, Jackson, FL, 1993.
- [24] R.L. Edwards, H. Cheng, M.T. Murrell, S.J. Goldstein, Protactinium-231 dating of carbonates by thermal ionization mass spectrometry implications for quaternary climate change, *Science* 276 (1997) 782–786.
- [25] F.W. Taylor, P. Mann, Late Quaternary folding of coral reef terraces, Barbados, *Geology* 19 (1991) 103–106.
- [26] E. Bard, R.G. Fairbanks, B. Hamelin, A. Zindler, H. Chi Trach, Uranium-234 anomalies in corals older than 150 000 years, *Geochim. Cosmochim. Acta* 55 (1991) 2385–2390.
- [27] W.X. Li, J. Lundberg, A.P. Dickin, D.C. Ford, H.P. Schwarcz, R.H. McNutt, D. Williams, High-precision mass-spectrometric uranium-series dating of cave deposits and implications for palaeoclimate studies, *Nature* 339 (1989) 534–536.
- [28] J. Lundberg, D.C. Ford, Late Pleistocene sea level change in the Bahamas from mass spectrometric U-series dating of submerged speleothem, *Quat. Sci. Rev.* 13 (1994) 1–14.
- [29] D.A. Richards, P.L. Smart, R.I. Edwards, Late Pleistocene sea-level change based on high-precision mass-spectrometric  $^{230}\text{Th}$  ages of submerged speleothems from the Bahamas, *EOS* 73 (1992) 172.
- [30] P.L. Smart, D.A. Richards, R.L. Edwards, Uranium-series ages of speleothems from South Andros, Bahamas; implications for Quaternary sea-level history and palaeoclimate, *Cave Karst Sci.* 25 (1998) 67–74.
- [31] E. Bard, F. Antonioli, S. Silenzi, Timing of the penultimate interglacial and the astronomical theory of palaeoclimate, *Earth Planet. Sci. Lett.* (2002) in press.
- [32] W.S. Broecker, G.M. Henderson, The sequence of events surrounding Termination II and their implications for the cause of glacial–interglacial  $\text{CO}_2$  changes, *Paleoceanography* 13 (1998) 352–364.
- [33] B. Karner, J. Levine, B.P. Medeiros, R.A. Muller, A stacked benthic O-18 record, *Paleoceanography* (2002) submitted for publication.
- [34] E. Bard, B. Hamelin, R.G. Fairbanks, A. Zindler, Calibration of the C-14 timescale over the past 30 000 years using mass spectrometric U–Th ages from Barbados corals, *Nature* 345 (1990) 405–409.
- [35] M. Raymo, The timing of major climate terminations, *Paleoceanography* 12 (1997) 577–585.
- [36] S.J. Burns, D. Fleitmann, A. Matter, U. Neff, A. Mangini, Speleothem evidence from Oman for continental pluvial events during interglacial periods, *Geology* 29 (2001) 623–626.
- [37] J.L. Banner, G.J. Wasserburg, J.H. Chen, J.D. Humphrey, Uranium-series evidence on diagenesis and hydrology in Pleistocene carbonates of Barbados, West Indies, *Earth Planet. Sci. Lett.* 107 (1991) 129–137.
- [38] A.N. Dia, A.S. Cohen, R.K. O’Nions, J.A. Jackson, Rates of uplift investigated through  $^{230}\text{Th}$  dating in the Gulf of Corinth (Greece), *Chem. Geol.* 138 (1997) 171–184.
- [39] K.R. Ludwig, B.J. Szabo, J.G. Moore, K.R. Simmons, Crustal subsidence rate off Hawaii determined from  $^{234}\text{U}/^{238}\text{U}$  ages of drowned coral reefs, *Geology* 19 (1991) 171–174.
- [40] N.J. Shackleton, The 100 000-year ice-age cycle identified and found to lag temperature, carbon dioxide, and orbital eccentricity, *Science* 289 (2000) 1897–1902.
- [41] J.H. Chen, R.L. Edwards, G.J. Wasserburg,  $^{238}\text{U}$ ,  $^{234}\text{U}$  and  $^{232}\text{Th}$  in seawater, *Earth Planet. Sci. Lett.* 80 (1986) 241–251.
- [42] M.T. McCulloch, T. Esat, D. Weis, D.J. DePaolo, The coral record of last interglacial sea levels and sea surface temperatures, *Chem. Geol.* 169 (2000) 107–129.
- [43] S.J. Goldstein, M.T. Murrell, D.R. Janecky, Th and U isotopic systematics of basalts from the Juan de Fuca and Gorda Ridges by mass spectrometry, *Earth Planet. Sci. Lett.* 96 (1989) 134–146.
- [44] M. Malone, Geochemistry and mineralogy of periplatform carbonate sediments: Sites 1006, 1008, and 1009, in: P.K. Swart, G.P. Eberli, M.J. Malone, J.F. Sarg (Eds.), *Proc. Ocean Drilling Program, Scientific Results* 166, 2000, pp. 145–152.